



Published in final edited form as:

*Conf Proc IEEE Eng Med Biol Soc.* 2009 ; 2009: 1616–1618. doi:10.1109/IEMBS.2009.5333221.

## Insertion of a Three Dimensional Silicon Microelectrode Assembly through a Thick Meningeal Membrane

Taneev Escamilla-Mackert, Nicholas B. Langhals [Member, IEEE], Takashi D. Y. Kozai, and Daryl R. Kipke [Member, IEEE]

University of Michigan Department of Biomedical Engineering, Ann Arbor, MI 48109 USA, 734-764-3716; fax: 734-647-4834

Daryl R. Kipke: dkipke@umich.edu

### Abstract

There are many different needs for intraoperative mapping in both rodent as well as human situations. Whether the goal of the procedure is for epileptic mapping, removal of cancerous tissue, mapping the motor and sensory cortices, or understanding the underlying neural networks within the brain, dense three-dimensional electrode arrays are necessary. In this study, we outlined and validated thicker silicon probe designs for use in intracortical mapping applications. Multiple shank and electrode site configurations were implanted successfully through rat dura as a model for human pia, and all devices maintained the electrical functionality necessary for electrophysiological mapping applications.

### I. INTRODUCTION

Neuronal ensembles dictate functions such as memory, behavior, cognition, and can even cause disease. The first step towards understanding how the brain works is to understand the anatomical structures through mapping of brain regions [1]. Many research and clinical applications for understanding brain structure and function require an implantable microstructure capable of sampling or influencing neural activity from localized populations of neurons [2, 3]. Significant challenges remain in the development of implantable devices for multidimensional human intracortical mapping. While current designs are limited to one single plane of sampling, and either high-insertion speeds or the resection of meninges prior to insertion, new devices are being developed to address these limitations and optimize insertion techniques for implantable 3D arrays [4–7]. Three-dimensional mapping with planar microfabricated technology enables new research thrusts in rodent and eventually human intracortical and intraoperative mapping. Human implantation of mapping microelectrodes typically involves the removal of the dura and possibly the pia mater. However, resection of the underlying pia mater results in increased damage to the underlying cortical tissue with a direct correlation to patient risk[2].

The goal of this study was to validate the potential of this planar silicon probe technology for insertion through the thick meningeal membrane in rat while remaining physically intact and electrically viable following insertion. The rat dura was used as an adequate model for the human pia as it has a similar thickness and tensile strength to the human pia mater. Human pia ranges from 15 to 100  $\mu\text{m}$  [8–10], while the cranial rat dura is  $\sim 80\mu\text{m}$ [11]. Also,

the tensile strength of rat dura ranges from 660–1270 kPa [9], while human pia is typically 600–3000 kPa [8–10]. Due to these similarities, penetrating through the rat dura provided a comparable model for penetrating the human pia. These specifications were evaluated and characterized through insertion tests and electrophysiological recordings in a rat model. While a functional version of a thick silicon 3D probe was not used in this study, efforts to assemble these thicker-technology devices into functional prototypes for intracortical mapping applications are underway.

## II. Methods

### A. Microelectrodes

The micromachined silicon probes used in this experiment were provided by NeuroNexus Technologies, Inc., (Ann Arbor, MI). These probes were fabricated using a modified technique resulting in devices that are 50  $\mu\text{m}$  thick, much larger than the typical 15  $\mu\text{m}$  devices. This increased thickness resulted in increased stiffness, strength, and an incorporated tapered tip, which made these devices better optimized for insertion through the rat dura. During this experiment, probe designs consisted of multiple shanks and site orientations. Specifications of the designs used in this study are presented in Table 1 and displayed in Fig. 1.

### B. Surgical Procedure

All probes were implanted in four Sprague Dawley rats using similar experimental procedures outlined previously [12]. The animals were administered general anesthesia (mixture of 50 mg/mL ketamine, 5 mg/mL xylazine, and 1 mg/mL acepromazine), using intraperitoneal injection with an initial dosage of 0.1 mL/100 g body weight and maintained throughout the surgical procedure using regular supplements of ketamine as needed. Each animal was mounted to a standard stereotaxic frame, and a craniotomy (approximately 3 by 5 mm) was made in the left hemisphere spaced between lamda and bregma. The dura was left intact with no observable incisions. The cortical surface was kept moist by irrigating with 0.9% sterile saline, and covered with saline-saturated GelFoam® (Henry Schein, Inc., Miami, FL).

All arrays, except the non-functional 3D, were inserted using a computer-controlled Precision Linear Actuator (P/N M-230.25, Polytec PI, Karlsruhe, Germany). This insertion motor was affixed to the stereotaxic frame and was used to insert the neural probes to a depth of 2 mm at a rate of 1.2 mm/s using the maximum possible acceleration of the motor. The 3D probe was hand inserted with a micromanipulator until the array penetrated the dura to a final depth of 4 mm below the cortical surface. All probe insertions avoided any major surface vasculature. All procedures complied with the United States Department of Agriculture guidelines for the care and use of laboratory animals and were approved by the University of Michigan Committee on Use and Care of Animals.

### C. Neural Recordings

Following the craniotomy, subjects were moved to a Faraday cage and neural recordings were collected from animals to assess the viability of the probe following insertion. Each

probe remained inserted and was recorded for 20 minute segments, at which point the electrode was removed using the insertion motor and the next insertion took place. Signals were buffered using a 16-channel headstage amplifier, anti-aliasing filtered, amplified, and digitized before being stored for offline analysis. High speed data was collected from individual probes using a TDT multi-channel system (RX5, Tucker-Davis Technologies, Alachua, FL). Single and multi-unit recordings were sampled at ~25 kHz and bandpass filtered from 2–5000 Hz. Offline analysis was completed using custom automated MATLAB (Mathworks Inc., MA) software as reported previously [12, 13]. Briefly, candidate waveforms were selected and removed from full data traces using amplitude threshold discrimination windows. If a trace exceeded a threshold of 3.5 standard deviations, candidate waveforms were removed from the original trace for noise calculations. After candidate waveforms were removed, the noise level was defined as six times the standard deviation of the remaining signal. All waveforms were clustered using a fuzzy c-means technique, and the average waveform was calculated from the clustered signals. The signal-to-noise ratio was then determined by dividing the peak-to-peak spike amplitude of the mean waveform by the noise level for the respective channel.

### III. Results

Within this study multiple thick planar silicon probe designs were characterized and tested. The goal of these tests was to examine the feasibility of using these designs for successfully inserting through the thick rat meningeal membrane without fracturing while remaining electrically viable. Fig. 2 depicts time-lapse photography images extracted from real-time insertion videos of the different probe designs being inserted into the rat brain. While slight dimpling did occur during the insertion of all probe designs, insertion of the 3D probe resulted in the deepest indentation of the rat dura prior to penetration. All probes remained electrically functional after insertion through the rat dura as evidenced by the spike waveforms shown in Fig. 3. Multiple units were recorded from all inserted devices and multiple spikes were recorded on the same channel. On the tetrode device, similar waveforms were recorded on neighboring sites, most likely indicative of the same unit being recorded on the closely spaced electrodes.

### IV. Discussion

The ultimate goal of this work is to successfully develop and validate a technology platform that is capable of three-dimensional intracortical mapping in human patients. Within this study, we successfully validated a design concept of penetrating the rat dura as a model for human pia without fracturing and remaining electrical viable following insertion. With all multi-shank and 3D array designs, there is a greater potential for increased tissue damage. This damage may be caused by the increased force to penetrate dura or from the increased volume of cortical tissue that is displaced by the electrode array [4]. Further improvements in design and insertion methods could minimize the increased insertion damage.

The use of a thicker silicon probe technology was validated within this study. While a functional version of a thick silicon 3D probe was available, a companion study using the thin technology has recently been completed and efforts are underway to assemble the

thicker technology devices into functional prototypes for intracortical mapping applications. While these thinner devices are able to sample from a large 3D volume of neural tissue, they lack the strength necessary to penetrate the human pia or rat dura. There are many needs for intraoperative mapping in both rodent as well as human situations that require devices with both universal and application-specific qualities. Regardless of whether the goal of the procedure is for epileptic resection, removal of cancerous tissue, studying the motor and sensory cortices, or understanding the underlying neural networks within the brain, dense three-dimensional electrode arrays are a necessity.

## Acknowledgments

The authors would like to thank Dr. Kip Ludwig for paper review and editing as well as the rest of Neural Engineering Lab at the University of Michigan. N.B Langhals is a consultant for Neuronexus Technologies and D.R Kipke has a significant financial interest in NeuroNexus Technologies.

This work was supported in part by the Center for Neural Communication Technology - a P41 Resource Center funded by the National Institute of Biomedical Imaging and Bioengineering (NIBIB, P41 EB002030) and supported by the National Institutes of Health (NIH). This work was also supported by the University of Michigan Department of Biomedical Engineering Coulter Translational Research Partnership Award.

## VI. References

1. Kotter R, Wanke E. Mapping brains without coordinates. *Philos Trans R Soc Lond B Biol Sci.* Apr 29; 2005 360(1456):751–66. [PubMed: 15971361]
2. Kondziolka D. Complications of stereotactic brain surgery. *Neurologic clinics.* 1998; 16(1):35. [PubMed: 9421540]
3. Mazziotta JC, Toga AW, Evans A, Fox P, Lancaster J. A probabilistic atlas of the human brain: theory and rationale for its development. *The International Consortium for Brain Mapping (ICBM). Neuroimage.* Jun; 1995 2(2):89–101. [PubMed: 9343592]
4. Du J, Riedel-Kruse IH, Nawroth JC, Roukes ML, Laurent G, Masmanidis SC. High-resolution three-dimensional extracellular recording of neuronal activity with microfabricated electrode arrays. *J Neurophysiol.* Mar; 2009 101(3):1671–8. [PubMed: 19091921]
5. Wise KD. Microelectrodes, Microelectronics, and Implantable Neural Microsystems. *Proceedings of the IEEE.* 2008; 96(7):1184.
6. Rousche PJ, Normann RA. Chronic recording capability of the Utah Intracortical Electrode Array in cat sensory cortex. *J Neurosci Methods.* Jul 1; 1998 82(1):1–15. [PubMed: 10223510]
7. Ulbert I, Halgren E, Heit G, Karmos G. Multiple microelectrode-recording system for human intracortical applications. *J Neurosci Methods.* Mar 30; 2001 106(1):69–79. [PubMed: 11248342]
8. Reina MA, De Leon Casasola L, de O, Villanueva MC, Lopez A, Maches F, De Andres JA. Ultrastructural findings in human spinal pia mater in relation to subarachnoid anesthesia. *Anesth Analg.* May; 2004 98(5):1479–85. table of contents. [PubMed: 15105235]
9. Sparrey CJ, Manley GT, Keaveny TM. Effects of white, grey, and pia mater properties on tissue level stresses and strains in the compressed spinal cord. *J Neurotrauma.* Apr; 2009 26(4):585–95. [PubMed: 19292657]
10. Wittek A, Kikinis R, Warfield SK, Miller K. Brain shift computation using a fully nonlinear biomechanical model. *Med Image Comput Comput Assist Interv Int Conf Med Image Comput Comput Assist Interv.* 2005; 8(Pt 2):583–90.
11. Maikos JT, Elias RA, Shreiber DI. Mechanical properties of dura mater from the rat brain and spinal cord. *J Neurotrauma.* Jan; 2008 25(1):38–51. [PubMed: 18355157]
12. Ludwig KA, Miriani RM, Langhals NB, Joseph MD, Anderson DJ, Kipke DR. Using a common average reference to improve cortical neuron recordings from microelectrode arrays. *J Neurophysiol.* Mar; 2009 101(3):1679–89. [PubMed: 19109453]

13. Ludwig KA, Uram JD, Yang J, Martin DC, Kipke DR. Chronic neural recordings using silicon microelectrode arrays electrochemically deposited with a poly(3,4-ethylenedioxythiophene) (PEDOT) film. *J Neural Eng.* Mar; 2006 3(1):59–70. [PubMed: 16510943]

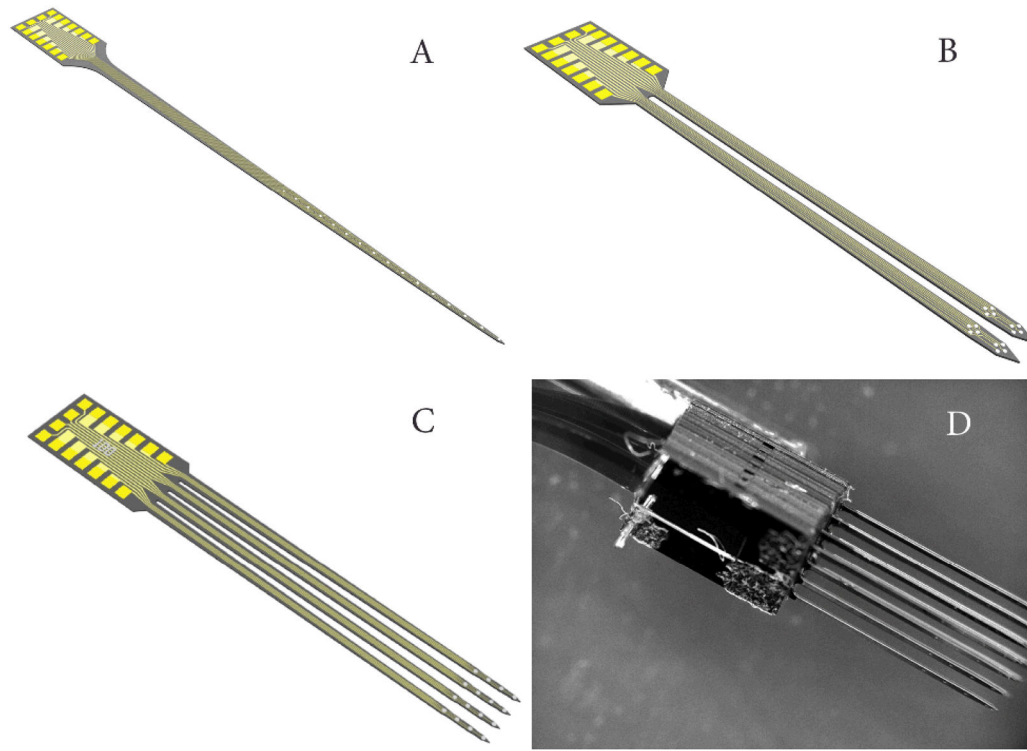


**Figure 1.**

All the devices were fabricated 50 microns thick A) Single shank design B) two-shank design C) Four-shank design D) 3D probe (4X4)

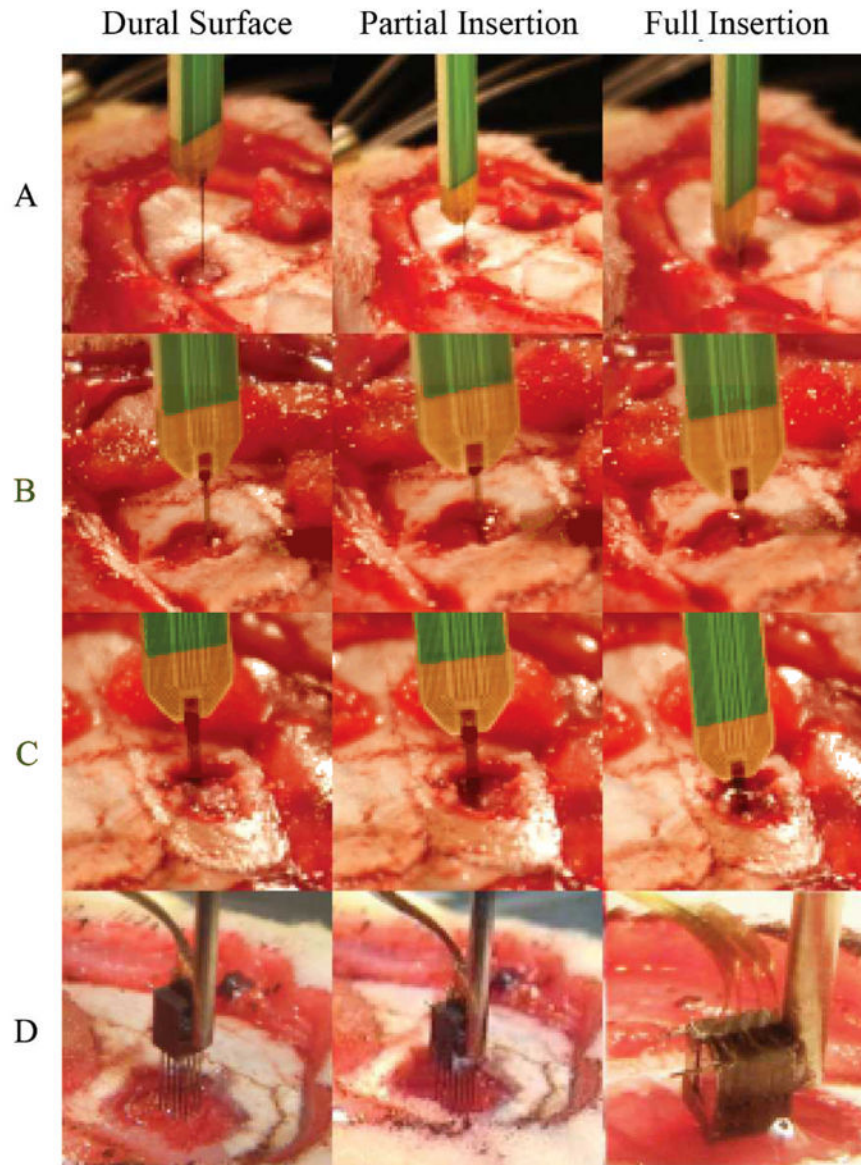


**Figure 2.**

Still-frame images of probe insertions into rat brain. a–c) Shanks 1, 2, 4 shank probes respectively, all inserted with minimal dimpling d) 3D probe inserted with increased dimpling

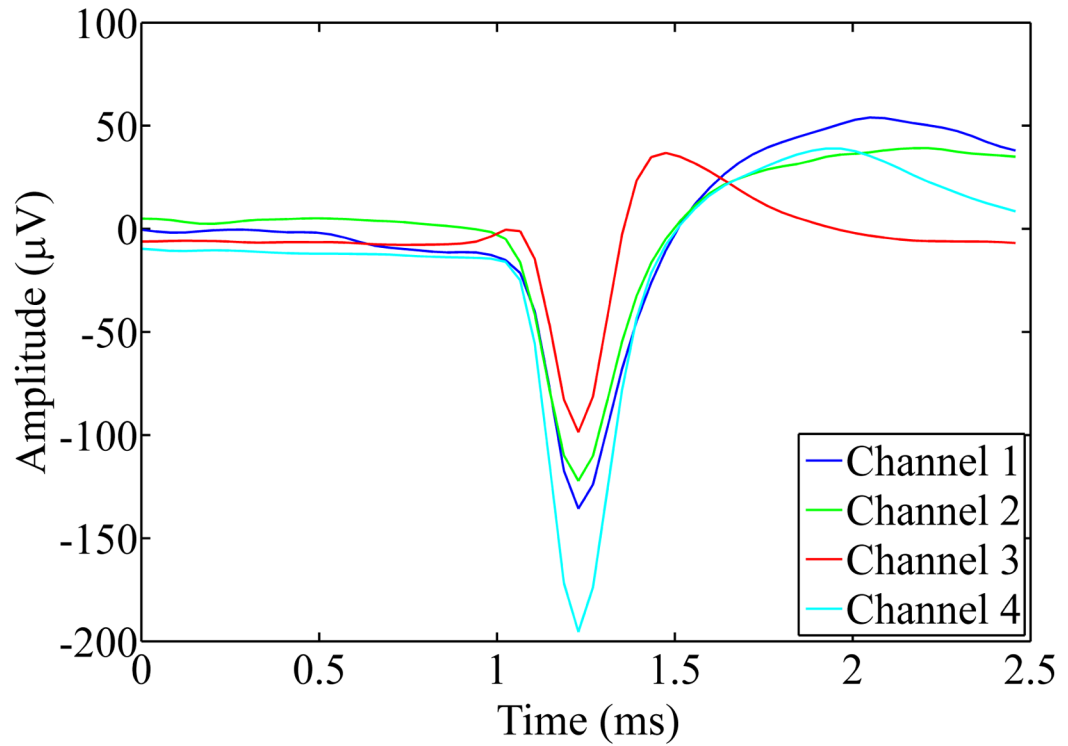


**Figure 3.**

Mean spike waveforms from an example tetrode recording session. Channels 1, 2, and 3 were from the same tetrode array, while channel 4 was from a different array on the same device. Signal to noise ratios were 1.5, 1.4, 1.1, and 1.9 respectively.



TABLE 1

## Microelectrodes

Shank Number	Shank Spacing	Length (mm)	Electrode Style	Site Spacing ( $\mu\text{m}$ )	Site Size ( $\mu\text{m}^2$ )
1	N/A	5	Single	150	413
2	150	3	Tetrode	35	312
4	100	3	Single	100	413
16-4X4(3D)	400	4	N/A	N/A	N/A